Sindh Univ. Res. Jour. (Sci. Ser.) Vol. 45 (3) 496-500 (2013)

SINDH UNIVERSITY RESEARCH JOURNAL (SCIENCE SERIES)

Modelling and Simulation of the Rotating Cavity flow system

A. F. ABBASI[++], M.U. MEMON, J. DAUDPOTO, A. H. BALOCH

Mehran University of Engineering and Technology Jamshoro, Sindh, Pakistan

Received 19th March 2013 and Revised 8st July 2013

Abstract: This paper presents the finite-difference solutions for a rotating disc flows system for the series of rotational Reynolds numbers $Re_{\square}=5.5\times10^5 \leq Re_{\square} \leq 1.1\times10^6$ at a fixed value of mass flow rate $C_w=2500$. In order to assess the performance level of the closures, two turbulence models: the low Reynolds number k-ε model and low Reynolds number second moment closure are employed to predict the basic characteristics of rotating disc flow system. Predicted results revealed the profound effects of higher rotational Reynolds number on the stream lines and tangential velocity profiles, particularly in the source and sinks regions. The comparison of the two models shows that the low Reynolds number second moment closure produces a better agreement with the measurements in the central core region of the cavity.

Keywords: Rotating cavity system, Low Reynolds number, Second moment closure

1. INTRODUCTION

The continual advancement in the gas turbine engines has enhanced the scope of operating conditions that result in the amplification of the turbine entry temperature to over 1600°C as reported by the (Rolls-Royce, 2005). Therefore, the understanding of the fluid flow and heat transfer processes occurring in the gas turbine engines is of primary interest which helps the turbomachinery community, to calculate the accurate quantity of internal cooling air for the gas turbine engines. This air extracted from the compressor stages at the penalty of useful fuel burning. (Childs, *et al.,* 2006) point out that about 20% of the engine core flow air is bled from the compressor stages for the cooling of different components of the engine, which estimated about 5% of fuel consumption. Thus, it is necessary to estimate the correct amount of cooling air and to improve the performance of the gas turbine engine. The rotating cavity system is frequently employed in the gas turbine engines for the internal air cooling applications. This system of geometry is formed between the two discs, rotating in the same direction so-called rotating cavity system. The significant scope of the problem has motivated the many research workers to dedicate their efforts to this area of interest. Earlier research work revealed that the fluid flow at the constant temperature within the two corotating discs is similar to the isothermal flow. The identical flow effects were showed in the research papers authored by (Owen, *et al.,* 2007, 2011; Serre, *et al.,* 2001; Owen and Roger, 1995; Memon, 1995; Schiestel, *et al.,* 1993). Moreover, (Pincombe, 1983; Morse, 1988; Gan, *et al.,* 1996; Soong, *et al.,* 2003; Randriamampianina, *et al.,* 2004) carried out the experimental and numerical studies to investigate the fluid flow behavior in the rotating cavity system. These studies conclude that the parametric effects are of paramount interest and altered the flow structure within the cavity. Therefore, it is important to investigate the characteristics of fluid flow behaviour in the rotating discs flow system. The two low Reynolds number turbulence models, the k-ε model and the Reynolds Stress model have been employed to assess the main characteristics of the flow. The predicted results have been validated with the experimental data of (Owen, *et al.,* 1985) and showed a good level of agreement.

2. GEOMETERICAL CONFIGURATION AND BOUNDARY CONDITIONS

The geometry of the complex system has been presented through a simplified geometrical configuration, as shown in **(Fig. 1)**. The simplified geometry and inlet and out let boundary conditions are identical to pertinent experimental geometry of (Owen, *et al.,* 1985).The geometrical dimensions and boundary conditions are given as under:

b=0.2m s=0.02m, and G = 0.1

$U=V=W=0$	at $z=0$, $r_i<r<b$,
$V=W=0$, $U=U_i$	at $z=0$, $0<r<r_i$,
$U=V=0$, $W=\Omega r$	at $z=s$, $0<r<b$
$U=W=0$, $V=V_o$	at $r=b$, $0<z<s_c$,

[++]Corresponding author, e-mail address: afatah66@yahoo.com, contact #03003793045

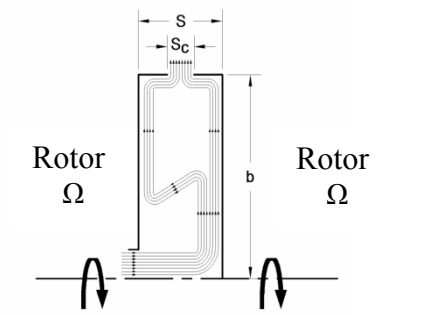


Fig. 1 Schematic diagram for rotating cavity system with Radial outflow

3. TURBULENCE MODELING

Two low Reynolds number turbulence models, k-ε model and Reynolds Stress model have been implemented for the predictions. Both the models are classified according the modelling procedure of the Reynolds stress components.

3.1 Low Reynolds number k-ε model

In order to solve the turbulence quantities, the low Reynolds number k-ε model of (Morse, 1991) has been adopted. This model is based on the transport equation for the kinetic energy (k) and its dissipation rate (ε).

$$\rho\overline{u_i u_j} = 2/3\delta_{ij}\rho k - \mu_T\left(\frac{\partial U_i}{\partial x_j} + \frac{\partial U_j}{\partial x_i} - 2/3\,\delta_{ij}\nabla.\underline{V}\right) \qquad 1$$

Where $\nabla.\underline{V}$ is the divergence of velocity vector,

$$\nabla.\underline{V} = \frac{\partial U}{\partial z} + \frac{\partial V}{\partial r} + \frac{V}{r} \qquad (2)$$

$2/3\delta_{ij}$ = Kronecker delta (δ_{ij}) shows normal stresses (i.e. i=j only)

3.2 Low Reynolds number second moment closure

In this modelling procedure isotropic eddy viscosity components are not taken in account however, the transport equations are resolved for each Reynolds stress component. This modelling procedure commonly known as the low Reynolds number second moment closure (Memon, 1995), which is based on the suggestions of (Lai and So, 1990).

Following equation presents the exact governing equation of the Reynolds stress components,

$$\frac{\partial}{\partial x_k}\left(\rho U_k\overline{u_i u_j}\right) = \frac{\partial}{\partial x_k}\left(\mu\frac{\partial\overline{u_i u_j}}{\partial x_k}\right) + \frac{\partial}{\partial x_k}\left(-\rho\overline{u_i u_j u_k}\right) \qquad (3)$$
$$-\rho\left(\overline{u_j u_k}\frac{\partial U_i}{\partial x_k} + \overline{u_i u_k}\frac{\partial U_j}{\partial x_k}\right) - \overline{\left(u_i\frac{\partial p}{\partial x_j} + u_j\frac{\partial p}{\partial x_i}\right)} - 2\mu\overline{\frac{\partial u_i}{\partial x_k}\frac{\partial u_j}{\partial x_k}}$$

or symbolically as

$$C_{ij} = D^{v}_{ij} + D^{T}_{ij} + P_{ij} + \Pi_{ij} - \varepsilon_{ij} \qquad (4)$$

Component on left side can be read as convection and on right side as viscous diffusion, turbulent diffusion and production by mean strain, redistribution and diffusion due to the pressure interactions, and viscous dissipation of the Reynolds stresses respectively. As given in references (Memon, 1995; Lai and So, 1990).

4. COMPUTATIONAL PROCEDURE

Constant temperature predictions have been carried out through the computational procedure of TEACH, which is based on a Finite Volume Method. To solve the discretized transport equations, a line-by-line method has been adopted, which is supported by the Tri-Diagonal Matrix Algorithm (TDMA). The variables of transport equations are solved at the main grid nodes. However, the momentum equations are solved by adopting the staggered grid arrangement of (Harlow and Welch, 1965), as presented in **(Fig. 2)**. The SIMPLEC algorithm of (Van Doormal and Raithby, 1984) has been employed for the mass continuity and coupling of the pressure-velocity flow field. A non-uniform mesh arrangement (75x92) in the axial and radial directions has been employed, as demonstrated in **(Fig. 3)**. The unknown variables emerged in the algebraic equations are discretised at fixed number of grid points of the calculating domain. Therefore, two discretisation schemes, HYBRID and HOUS have been used in combined form for the mean and fluctuating components. The same set of schemes was used in the work of (Abbasi, *et al.,* 2012), (Memon, 1995) and (Morse, 1991) and provided the reliable and economical results.

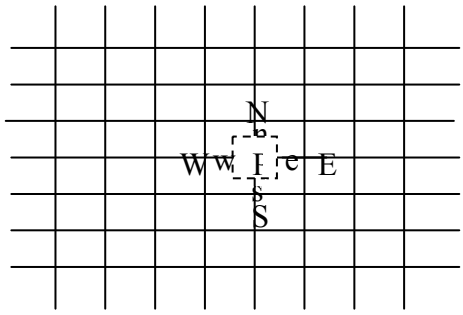


Fig.2 Staggered grid arrangements

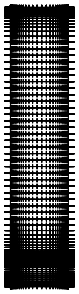


Fig. 3 Non-uniform grid

5 RESULTS AND DISCUSSION

The predicted results and there comparison with experimental data are presented in this section.

5.1 Computed Flow structure

The computed flow structures are presented for the series of rotational Reynolds number $5.5\times10^5 \leq Re_{\square} \leq 1.1\times10^6$ at a fixed mass flow rate C_w,=2500, as shown in **(Fig. 4)**. The computed stream lines of both models illustrate the four regions of the flows, source, sink, core and the Ekman layer. The incoming cooling air enters the cavity space through a central hole in the upstream disc and impinges on the downstream disc and developed a jet of fluid along the disc in radial direction known as wall-jet. The part of fluid flows in the reverse direction and forms a recirculating zone in the source region, in which all the components of the velocity in radial and axial direction became zero and remaining part of the fluid forms the Ekman boundary layers on both discs. Then the fluid redistributed in the sink region and formed recirculating cells of fluid in this region. The length and thickness of the wall-jet and source region is significantly affected by the rotational Reynolds number. For higher values of rotational Reynolds numbers, $Re_{\square}=8.2\times10^5$ and 1.1×10^6, the size of the source region decreased to 19% and 30% respectively. The decreased in the size of the source region has affected the intensity of the recirculating eddies and entraining boundary layers which is developed earlier on the upstream disc. Overall assessment of both models revealed that the source-sink regions are affected by the parameter rotational Reynolds number, as shown in **(Fig. 4)**.

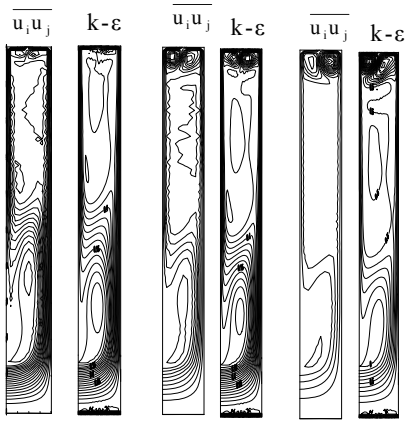


Fig. 4 Computed Flow structure for $5.5\times10^5 \leq Re_{\square} \leq 1.1\times10^6$ and Cw = 2500

5.2 Computed Velocity Profiles

To investigate the performance of two turbulence models, the effect of the rotational Reynolds number on the predicted tangential velocity profiles are presented for the range of rotational Reynolds numbers $5.5\times10^5 \leq Re_{\square} \leq 1.1\times10^6$, as shown in **(Fig. 5)**.The predictions of two models illustrated that for the lower value of Reynolds number, 5.5×10^5, the tangential velocity profile remains uniform in the source region up to radial location, r/b=0.5. However, for the higher rotational Reynolds numbers, $Re_{\square}=8.2\times10^5$ and 1.1×10^6, the radial extend of the uniform tangential velocity profiles decreased to r/b=0.4 and r/b=0.3 respectively. This revealed that the recirculation of fluid in the source region has been reduced at higher rotational Reynolds number, as shown in **(Fig. 5)**. This is also obvious from the corresponding flow structures predicted by the two models in (Fig. 4). After the source, there is steep variation in the tangential velocity profiles which is increased for the higher rotational speed. In the outer region of the cavity, the tangential velocity profiles further increased to the maximum level. The comparison of the two models illustrates that the low Reynolds number second moment closure shows a closer agreement with the measurements of (Owen, *et al.,* 1985). This closer agreement confirmed the robustness and the great scope of applicability of the low Reynolds number second moment closure. This developed the confidence of researchers to use this model reliably for more complex wall-bounded shear flows.

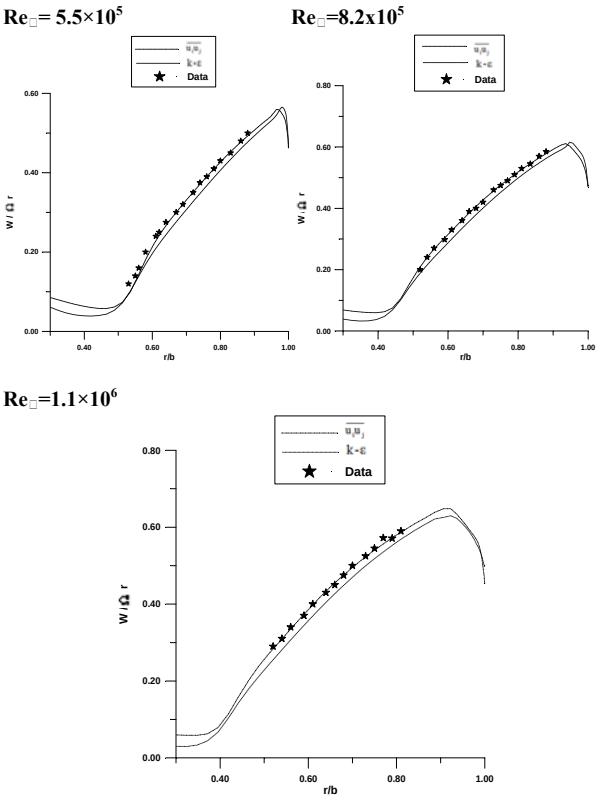


Fig. 5 Comparison of radial distribution of tangential velocity profiles for $5.5\times10^5 \leq Re_{\square} \leq 1.1\times10^6$For Cw = 2500

Table 1 Comparison between computed moment coefficient

Rotational Reynolds number (Re_θ)	Mass Flow rate (C_w)	Up-stream disc (C_mx 10^3)		Down-stream disc (C_mx 10^3)	
		k-ε	$\overline{u_i u_j}$	k-ε	$\overline{u_i u_j}$
$5.5x10^5$	2500	2.84	2.97	2.90	3.01
$8.2x10^5$	2500	2.12	2.23	2.15	2.24
$1.10x10^6$	2500	1.73	1.82	1.75	1.85

Further validation of predictions have been carried out by the comparison of computed moment coefficient of both models for the range of rotational Reynolds number $5.5\times10^5 \leq Re_{\square} \leq 1.1\times10^6$ at fixed mass flow rate, C_w=2500, as shown in **(Table 1).**

As mentioned in the previous subsection, the nature of the flow in the rotating cavity depends on the rotational Reynolds number and the mass flow rate. Therefore, parametric effects are obvious on the computed moment coefficients for both discs. These effects proposed that for the higher value of rotational Reynolds number, the wall-jet effect has decreased consequently, the lower value of moment coefficient has been predicted on both the discs. The reduction in the moment coefficient reveals the tendency of the flow symmetry on both the discs on higher rotational speed. It can be observed that the moment coefficient of the downstream disc predicted by the k-ε model and Reynolds stress model is slightly higher than the upstream disc; this signifies the impingement effect on the downstream disc. Unfortunately for this typical case of the rotating cavity flows, no experimental data is available for the validation moment coefficient. However, both models show the consistency in the predicted values of the moment coefficients. Overall, comparison of two models shows that the Reynolds stress model has predicted the slightly higher value of moment coefficient than that of the k-ε model for both discs. This trend of variation in moment coefficient confirms the sensitivity of the moment coefficient to the rotational Reynolds number.

6. CONCLUSIONS

The rotating cavity system has been investigated at isothermal conditions for the range of rotational Reynolds number $5.5\times10^5 \leq Re_{\square} \leq 1.1\times10^6$ at a constant mass flow rate C_w=2500. The significant effects of the rotational Reynolds number have been noted in the rotating cavity particularly, in the recirculating core region and source region. For the higher rotational Reynolds number, the size of the source and sink regions have been contracted and elongated respectively. This behaviour revealed that the recirculation level in the source region is decreased for the higher rotational speed. The computed moment coefficients have been affected by higher rotational Reynolds number, which is decreased monotonically for higher values rotational Reynolds numbers. This trend of variation in the moment coefficient attributed that the wall-jet effects are less influential for the higher rotational speed and formed the flow symmetry on both the discs. Overall comparison of both the models showed that the performance of the low Reynolds number second moment closure is better than the k-ε model, particularly in the more complex central core region.

7. NOMENCLATURE

b	outer radius of cavity
$C_m = M/(1/2\,\rho\Omega^2 b^5)$	moment coefficient
$C_w = \dot{m}/\mu b$	non-dimensional flow rate ()
G = s/b	cavity gap ratio
k	turbulent kinetic energy
M	frictional moment
$Re_\theta = \Omega b^2/\nu$	rotational Reynolds number
r	radial co-ordinate
r/b	non-dimensional radial co-ordinate
r_i	inner disc radius
s	axial gap between the discs
s_c	clearance between the disc and shroud
U,V,W	mean velocity components in z, r, θ direction
$\overline{u_i u_j}$	Reynolds stress tensor
z	axial co-ordinate
z/s	non-dimensional axial co-ordinate
ε	dissipation rate of turbulent kinetic energy
θ	circumferential co-ordinate
ν	kinematic viscosity
μ	dynamic viscosity
Ω	rotational speed of the disc
ρ	density
δ_{ij}	Kronecker delta
fd	free disc

ACKNOWLEDGEMENTS

This work acknowledges the support of Higher Education Commission, Government of Pakistan for providing financial assistance to fulfil this task. Authors are also thankful to the Mehran University of Engineering and Technology and Faculty members Department of Mechanical Engineering for their encouragement and moral support during the completion of this work.

REFRENCES:

Abbasi, A. F., M. D. Memon, and A. Baloch, (2012) "Modelling and Predictions of Isothermal Flow Inside the Closed Rotor-Stator Flows", Mehran University Research Journal of Engineering & Technology, Vol. 31**(1)**: 83-94.

Childs, P. R. N., K. Dullenkopf, and D. Bohn, (2006) Internal air systems experimental rig best practice. ASME Paper GT 2006-90215.

Gan, X., I. Mirzaee, J. M.,Owen, D.A.S. Rees, and M. Wilson, (1996) "Flow in a rotating cavity with a peripheral inlet and outlet of cooling air" , ASME Int. Gas Turbine and Aeroengine Cong., paper 96-GT-309, Birmingham.

Harlow, F. H. and J. E. Welch, (1965) "Numerical calculation of time-dependent viscous incompressible flow of fluid with free surface" Physics of Fluids 8: 2182-2189.

Lai, Y. G. and R.M.C. So, (1990) "On near-wall turbulent flow modelling", J. Fluid Mech. 221: 641-673.

Memon, M. D. (1995) "Numerical modelling and prediction of fluid flow and heat transfer in rotating disc geometries", D.Phil. Thesis. University of Sussex.

Morse, A. P. (1991) "Application of a low Reynolds number k-ε turbulence model to high-speed rotating cavity flows", J. Turbomachinery. 113: 98-105.

Morse, A. P. (1988) "Numerical prediction of turbulent flow in rotating cavities" J. Turbomachinery. 110: 202-211.

Owen, J. M. (2011) "Prediction of ingestion through turbine rim seals—Part I: Rotationally Induced Ingress", J. Turbomachinery, vol. 133, 031005-1-031005-9

Owen, J. M., H.Abrahamsson, and K . Lindblad, (2007) "Buoyancy-Induced Flow in Open Rotating Cavities" ASME J. Eng. Gas Turbines Power. 129 **(4):** 893–900.

Owen J. M. and R. H. Rogers (1995) "Rotating cavities, Flow and Heat Transfer in Rotating Disc Systems 2, Rotating cavities", Research Studies Press/John Wiley Inc. New York.

Owen, J. M., J. R. Pincombe, and R. H Roger. (1985) "Source-sink flow inside a rotating cylindrical cavity", J. Fluid Mech. 155: 233-265.

Pincombe, J. R. (1983) "Optical measurements of the flow inside a rotating cylinder", D.Phil. Thesis. University of Sussex.

Randriamampianina, A., R. Schiestel, and M. Wilson, (2004) "The turbulent flow in an enclosed corotating disk pair: axisymmetric numerical simulation and Reynolds stress modelling", Int. J. Heat and Fluid Flow. 25: 897-914.

Rolls-Royce (2005) The Jet Engine, Rolls-Royce Publications.

Schiestel, R., L. Elena, and T.Rezoug, (1993) "Numerical modelling of turbulent flow and heat transfer in rotating cavities", Numerical Heat Transfer. Part A-Applications. 24: 45-55.

Soong, C.Y. C.C.Wu, and T. P. Liu, (2003) "Flow structure between two co-axial discs rotating independently", Experimental Thermal and Fluid science. 27: 295-311.

Serre, E., Crespo DEL Aroco and P. Bontoux, (2001) "Annular and spiral patterns in flows between rotating and stationary discs", J. Fluid Mech. 434: 65-100.

Van, D. J. P. and G. D. Raithby, (1984) "Enhancement of the SIMPLE method for predicting incompressible fluid flow" Num. Heat Transfer. 7, 147-163.